Concentration Polarization at Langmuir Monolayer Deposition: The Role of Indifferent Electrolytes

M. P. Bondarenko,[†] V. I. Kovalchuk,[†] E. K. Zholkovskiy,[†] and D. Vollhardt*[,‡]

Institute of Biocolloid Chemistry of NAS of Ukraine, Vernadskogo 42, 03142, Kiev, Ukraine, and Max Planck Institute of Colloids and Interfaces, D-14424 Potsdam/Golm, Germany

Received: April 21, 2006; In Final Form: November 2, 2006

Under dynamic conditions of the charged Langmuir monolayer deposition onto a substrate surface, ion concentration and electric potential profiles are induced in the subphase around the three-phase contact line. Such local changes in the subphase influence the deposition process, particularly the monolayer adhesion work and the maximum deposition rate. If indifferent electrolytes (not interacting chemically with interfacial groups) are present in the solutions, they can affect electric potential distributions and therefore the monolayer charge and the deposition process as a whole. With increasing deposition rate, the indifferent electrolyte counterions replace gradually the potential-determining counterions in a close vicinity to the contact line. This leads to increasing monolayer ionization and increasing electrostatic repulsion between the monolayer and substrate. When the deposition rate approaches the critical one, the charge of the monolayer increases dramatically and the stationary monolayer deposition becomes impossible. Such a significant increase of the monolayer charge is not observed in the absence of indifferent electrolytes.

1. Introduction

Laterally structured surfaces with controlled anisotropic physical and chemical properties are of increased interest in modern science. It is shown in a number of recent studies (refs 1−6 and the references therein) that the well-known Langmuir−Blodgett (LB) technique is an efficient way toward the fabrication of laterally patterned structures on solid supports. Such patterned structures (e.g., uniform stripes and striations) with properties controlled on the micro- or nanometer scale can be formed under certain experimental conditions as a result of wetting instabilities during LB film transfer. Therefore, the phenomena of instability during the deposition of LB films are the focus of many recent studies.[1−6]

Recently, we considered a new electrokinetic mechanism that can lead to meniscus instability and stripe pattern formation when a charged Langmuir monolayer is deposited onto a solid substrate.[7,8] When withdrawing the substrate, the monolayer is always deposited in the electroneutral state. At the same time, being in contact with the electrolyte solution (subphase), some monolayers bear electric charge due to dissociation of the interfacial groups. Considering the charge and mass balances during the charged monolayer deposition leads to the conclusion that, in the solution near the three-phase contact line, both the electric field and the ion concentration profiles are created.[9−11]

Such electric and concentration fields depend on the deposition rate.[11] When increasing the transfer rate, the concentration profiles become sharper and the ionic fluxes, which restore the steady-state ionic balance, increase. For sufficiently high deposition rates, the subphase composition substantially changes in the immediate vicinity of the contact line. The predicted changes in the subphase composition (concentration polarization) can drastically affect the adhesion work and thus the dynamic contact angle. When the deposition rate approaches a critical value, the adhesion work approaches zero. The latter leads to disruption of the monolayer deposition.

The experimental data show that the maximum deposition rate strongly depends on the ionic composition of the bulk solution. For negatively charged fatty acid monolayers, the maximum deposition rate in the presence of bivalent counterions, which can form complexes with the interfacial ionized groups, is higher than in the absence of the counterions and increases with decreasing pH.[12−15] For positively charged fatty amine monolayers, the maximum deposition rate also increases when bivalent counterions, that can be bound at the interface, are added to the subphase.[12−14,16] The experimental data agree with the behavior predicted from the consideration of changes in the subphase composition near the contact line.[11]

Some of the experimental and theoretical results point out that the indifferent electrolytes can affect the deposition of charged Langmuir monolayers (e.g., sodium salts in the case of fatty acid monolayers). In contrast to potential-determining counterions, the ions of indifferent electrolytes do not interact chemically with interfacial groups. However, if indifferent electrolytes are present in the solutions, they can affect electric potential distributions and therefore the monolayer charge and the deposition process as a whole. The diffuse layer thickness decreases when the indifferent electrolyte concentration in the solution increases, which should reduce the electrostatic repulsion between the monolayer and substrate surface. However, in contrast to the case of potential-determining counterions, this does not lead to an increase in the maximum deposition rate.[12,13] Instead, the maximum deposition rate decreases with increasing indifferent electrolyte concentration.[15] It is also known that the deposition of a fatty acid monolayer from sodium salt solutions is impossible if the potential-determining counterions (hydrogen or bivalent metal ions) are removed.[12,17]

In our previous study, it was shown that, to provide steady-state ion balance during a charged monolayer deposition, the

* Corresponding author.
[†] Institute of Biocolloid Chemistry of NAS of Ukraine.
[‡] Max Planck Institute of Colloids and Interfaces.

10.1021/jp062466v CCC: $37.00
Published on Web 01/30/2007

counterions of an indifferent electrolyte should be concentrated in the regions around the contact line.[10] When increasing the substrate speed, the counterions of indifferent electrolytes gradually replace the potential-determining ions in these regions. As a result, the surface charge density increases, and the electrostatic repulsion opposes the monolayer deposition. Thus, additions of indifferent electrolytes should lead to a stronger concentration polarization and therefore to a lower maximum deposition rate.

In ref 10, we analyzed the steady-state ion balance in the solution around the contact line assuming low magnitudes of both velocity and gradients of concentrations. The corresponding simplifications allow us to obtain some important qualitative conclusions about the effect of the bulk ion concentrations on the maximum deposition rate. However, using such an approximation, it is impossible to describe the dependencies of ion concentration profiles and respective electrodiffusion ion fluxes on the deposition rate. Therefore, the approach of ref 10 does not allow us to obtain the local subphase composition in the immediate vicinity of the contact line as a function of the deposition rate. The latter function is especially important for the analysis of the meniscus stability because the local subphase composition defines the charge and adhesion work of the monolayer.[10] In ref 11, we developed the general mathematical model that is capable of addressing the ion transfer in the vicinity of the contact line at high rates of LB deposition. The model developed in ref 11 is valid for arbitrary ionic systems. In the present study, we apply the developed model for describing the behavior of a system containing one monovalent potential-determining counterion and one monovalent indifferent counterion in the subphase at deposition rates ranging up to the critical value. The system considered here is the simplest model system where the effect of indifferent electrolytes is not complicated by other effects. However, the indifferent electrolytes should have the same influence on the meniscus stability and critical transfer rate for any charged monolayer deposition, and the results obtained for the simplest case are important for understanding the behavior of more complex systems.

2. Equilibrium Conditions

Let us consider a spread fatty acid monolayer in contact with a subphase containing two monovalent cations (e.g., hydrogen and sodium ions) and one monovalent anion. We assume that only one of the cations (hydrogen ion) can be bound to the negatively charged carboxylic groups of the monolayer and thus transferred with the monolayer to the substrate (Figure 1). This process can be described using the following equation of a reversible chemical reaction

$$RH \leftrightarrow R^- + H^+ \qquad (1)$$

The second cation (C^+) and the anion (A^-) are assumed to be not interacting with the monolayer and remaining in the solution.

The surface charge density and surface potential of such a monolayer depend on the ionic composition of the subphase (see Appendix). For an individual monolayer under equilibrium conditions, the behavior of the surface charge density $\sigma(C^0_{H^+}, C^0_{C^+})$ and surface potential $\varphi_S(C^0_{H^+}, C^0_{C^+})$ is illustrated in Figures 2 and 3 ($C^0_{H^+}$ and $C^0_{C^+}$ are the bulk concentrations of hydrogen ions and cations C^+, respectively). It is seen from Figure 2 that the surface charge density increases with subphase pH. For sufficiently high concentrations of $C^0_{C^+}$ (larger than 0.1 mol/m^3), the charge density increases with pH monotonously.

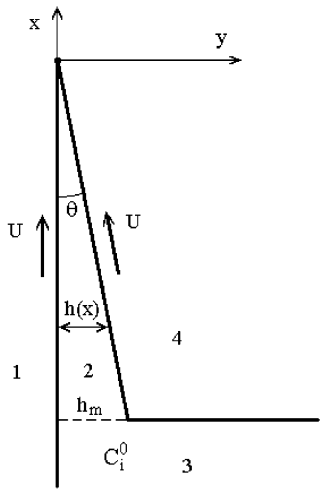

Figure 1. Sketch of the LB film deposition process (1, substrate; 2, meniscus region; 3, bulk solution; 4, air.

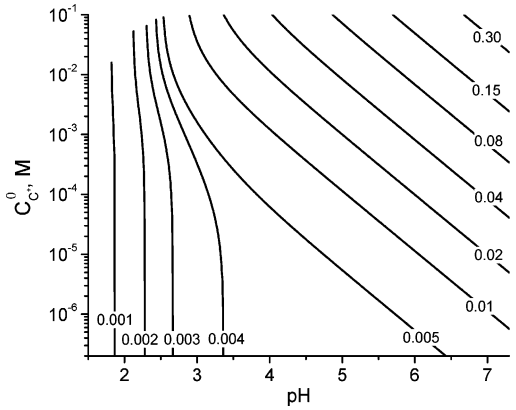

Figure 2. Equilibrium diagram of the surface charge density $\sigma(C^0_{H^+}, C^0_{C^+})$ for a fatty acid monolayer in the presence of an indifferent electrolyte. Lines of constant surface charge density (left to right, normalized by FX_R) correspond to 0.001, 0.002, 0.003, 0.004, 0.005, 0.01, 0.02, 0.04, 0.08, 0.15, and 0.30.

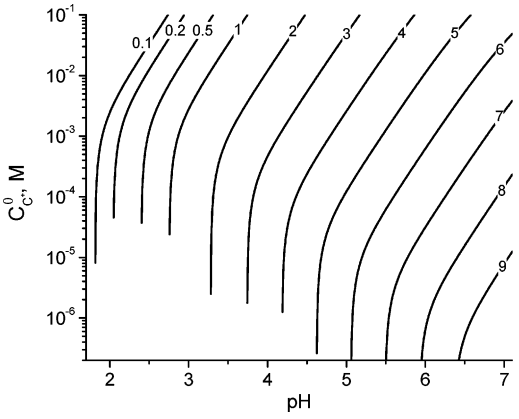

Figure 3. Equilibrium diagram of the surface potential $\varphi_S(C^0_{H^+}, C^0_{C^+})$ for a fatty acid monolayer in the presence of an indifferent electrolyte. Lines of constant surface potential (left to right, normalized by RT/F) correspond to 0.1, 0.2, 0.5, 1, 2, 3, 4, 5, 6, 7, 8, and 9.

For small concentrations of $C^0_{C^+}$, the increase of the charge density becomes slower at pH > 3.5, but then it accelerates again, when the concentration $C^0_{H^+}$ becomes smaller than $C^0_{C^+}$. At constant pH, the charge density increases with the indifferent electrolyte concentration $C^0_{C^+}$, when $C^0_{H^+} < C^0_{C^+}$, and is almost independent of $C^0_{C^+}$ in the opposite case. Thus, the potential-

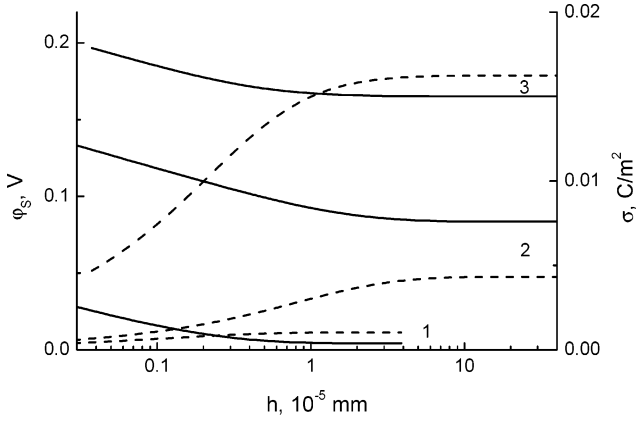

Figure 4. Variation of surface potential (full lines) and surface charge density (dashed lines) with the distance between the charged interfaces covered by fatty acid monolayers in the presence of an indifferent electrolyte ($C^0_{H^+} = 10^{-4}$ M) at different pH values in the subphase: pH = 2 (1), pH = 4 (2) and pH = 6 (3).

determining counterion concentration and the indifferent electrolyte concentration have an opposite effect on the charge density. However, their effect on the surface potential (Figure 3) is similar: the surface potential increases with a decrease of both concentrations $C^0_{H^+}$ and $C^0_{C^+}$.

In the region close to the contact line, the electric double layers formed at two charged interfaces overlap what results in a local increase of the electric potential.[9−11,19] The latter leads to an increase of the potential-determining counterion concentration in this region and to a shift of the chemical equilibrium according to eq 1 toward the formation of a neutral fatty acid. Consequently, the surface charge density decreases as the distance between the charged interfaces decreases. This is demonstrated by the results presented in Figure 4, as obtained from the solution of eqs A2, A4, and A5. The constant surface charge and constant surface potential represent two limiting cases for the behavior of a system with charge regulation.[18] The system considered here demonstrates an intermediate behavior. Toward the contact line, the surface charge density decreases whereas the surface potential increases. Immediately, at the contact line, the surface charge density tends to zero, and because of that, the electrostatic repulsion does not oppose the monolayer deposition.

3. Dynamic Conditions

3.1. Formulation of the Problem. During the monolayer transfer, a convective flow is induced in the solution around the contact line. Near the interfaces, the solution flow is directed toward the contact line. However, in the central part of the liquid film between the interfaces, the solution flow is directed outward from the contact line, because the solvent is practically not removed with the deposited monolayer. In the framework of the lubrication approximation, the velocity field can be described by the equation[20]

$$v(y) = U\left(-\frac{1}{2} + 6\left(\frac{y}{h} - \frac{1}{2}\right)^2\right) \tag{2}$$

where U is the velocity at the interfaces, y is the coordinate, directed normal to the film surfaces, and $h = h(x)$ is the local film thickness slowly changing with the coordinate x, directed along the film. The total volume flux through any cross-section of the film is zero: $\int_0^h v(y)\,dy = 0$.

In the presence of the above flow, the ith convective flux through a film cross-section is

$$J_i^C = \int_0^h v(y) C_i(x,y)\,dy \tag{3}$$

Because the ions within the diffuse layers are distributed nonuniformly, the convective fluxes of ions, given by eq 3, take nonzero values. The concentrations of counterions are larger at the interfaces than in the central part of the film. Therefore, their convective fluxes J_i^C are directed toward the contact line. In turn, the concentrations of coions decrease at the interfaces and their convective fluxes are directed outward the contact line.

The monolayer binds the counterions from the solution during the transfer onto the substrate surface. Under steady-state conditions, the flux of the potential-determining counterions H^+ should be equivalent to the flux of the oppositely charged surface groups through each of the solution cross-sections. Otherwise, the electroneutrality of the deposited film is violated. However, the convective flux of the potential-determining counterions alone is not sufficient for the complete neutralization of the surface charges during the deposition because (i) the counterions, distributed within the diffuse layers, move slower than the interfaces and a part of them returns back to the bulk solution with the back-flow in the central part of the film, and (ii) a part of counterions within the diffuse layers are the ions of indifferent electrolytes that do not bind at the monolayer. As a result, the potential-determining counterions are removed from the subphase at the contact line faster than they are supplied by the convective flux. Hence, around the contact line, their electrochemical potential decreases with respect to that in equilibrium.[9−11] In contrast, the counterions of an indifferent electrolyte C^+ are not removed from the subphase. Moreover, they are delivered to the contact line due to the convection. Thus, their electrochemical potential increases near the contact line. Consequently, with increasing deposition rate, the counterions of indifferent electrolytes gradually replace the potential-determining counterions in the subphase around the contact line. The electrochemical potential of coions, whose convective flux is directed outward from the contact line, decreases in this region.

In addition to ion convective fluxes, the above-described change of the electrochemical potentials of ions in the vicinity of the contact line leads to the appearance of electrodiffusion ion fluxes. During the monolayer transfer, the electrodiffusion fluxes, which restore the steady-state balance for each sort of the ions, are expressed as[10]

$$J^{ED}_{H^+}(x) = 2UX_{R^-}(x) - J^C_{H^+}(x) \tag{4}$$

$$J^{ED}_{C^+}(x) = -J^C_{C^+}(x) \tag{5}$$

$$J^{ED}_{A^-}(x) = -J^C_{A^-}(x) \tag{6}$$

where X_{R^-} is the interfacial molar concentration of the dissociated fatty acid and the J_i^C values are the convective fluxes of ions given by eq 3. Our objective is to obtain the distributions of ions $C_i(x,y)$, surface charge density $\sigma(x)$, and electric potential $\varphi(x,y)$ as well as the partial ion fluxes, given by eqs 4−6, under the conditions of steady-state monolayer transfer.

To simplify the analysis, similar to the previous papers,[10,11] we consider the case of small contact angles. In a thin liquid

film between monolayer and substrate surface, the equilibrium establishes much faster across the film than along it. This allows us to assume the electrochemical potentials of ions to be dependent on the x-coordinate only; i.e., the electrochemical potentials are assumed to be approximately constant across the film. Accordingly, the electrodiffusion ion fluxes can be approximated as

$$J_i^{ED}(x) = -D_i\int_0^h \frac{C_i(x,y)}{RT}\frac{\partial\mu_i^{el}}{\partial x}\,dy \approx -D_i\frac{\partial\mu_i^{el}}{\partial x}\int_0^h\frac{C_i(x,y)}{RT}\,dy \quad (7)$$

where $\mu_i^{el} = RT(z_i\varphi + \ln C_i)$ values are the electrochemical potentials of ions (in the ideal solution approximation) and the D_i values are the ion diffusion coefficients. The results, which are presented below, were obtained with the following diffusion coefficients: $D_{H^+} = 9.34 \times 10^{-9}$ m^2/s, $D_{A^-} = D_{Cl^-} = 2.04 \times 10^{-9}$ m^2/s, and $D_{C^+} = D_{Na^+} = 1.34 \times 10^{-9}$ m^2/s.

Assuming that local quasi-equilibrium holds across the film, we can also introduce the following variable substitution:[9,11]

$$C_i(x,y) = C_i^{qe}(x)\exp[-z_i\Psi(x,y)] \quad (8)$$

$$\varphi(x,y) = \Psi(x,y) + \Phi(x) \quad (9)$$

where $C_i^{qe}(x)$ values and $\Psi(x,y)$ are the quasi-equilibrium concentrations of ions and electric potential (dimensionless), respectively, and the potential $\Phi(x)$ is the difference between the actual and quasi-equilibrium electric potentials. For quasi-equilibrium concentrations, the same condition holds as for ion concentrations in an electroneutral bulk solution:

$$\sum_i z_i C_i^{qe} = 0 \quad (10)$$

With this condition, the number of independent new variables is the same as the number of initial variables. After substitution of the new variables into eqs 3−7 and accounting for eqs 2 and 10, one obtains a set of equations,[11] which for the case considered here takes the form

$$\frac{d\Phi}{dh} = \frac{U}{2\theta C_{A^-}^{qe}}\left[\frac{2X_{R^-}(h) - C_{H^+}^{qe}\beta^+(h)}{D_{H^+}\alpha^+(h)} - \frac{C_{C^+}^{qe}\beta^+(h)}{D_{C^+}\alpha^+(h)} + \frac{C_{A^-}^{qe}\beta^-(h)}{D_{A^-}\alpha^-(h)}\right] \quad (11)$$

$$\frac{d\ln C_{H^+}^{qe}}{dh} = \frac{U}{2\theta C_{A^-}^{qe}}\left[\frac{C_{C^+}^{qe} + C_{A^-}^{qe}}{C_{H^+}^{qe}}\times\frac{2X_{R^-}(h) - C_{H^+}^{qe}\beta^+(h)}{D_{H^+}\alpha^+(h)} + \frac{C_{C^+}^{qe}\beta^+(h)}{D_{C^+}\alpha^+(h)} - \frac{C_{A^-}^{qe}\beta^-(h)}{D_{A^-}\alpha^-(h)}\right] \quad (12)$$

$$\frac{d\ln C_{C^+}^{qe}}{dh} = \frac{U}{2\theta C_{A^-}^{qe}}\left[-\frac{2X_{R^-}(h) - C_{H^+}^{qe}\beta^+(h)}{D_{H^+}\alpha^+(h)} - \frac{(C_H^{+qe} + C_{A^-}^{qe})\beta^+(h)}{D_{C^+}\alpha^+(h)} - \frac{C_{A^-}^{qe}\beta^-(h)}{D_{A^-}\alpha^-(h)}\right] \quad (13)$$

$$\frac{d\ln C_{A^-}^{qe}}{dh} = \frac{U}{2\theta C_{A^-}^{qe}}\left[\frac{2X_{R^-}(h) - C_{H^+}^{qe}\beta^+(h)}{D_{H^+}\alpha^+(h)} - \frac{C_{C^-}^{qe}\beta^+(h)}{D_{C^+}\alpha^+(h)} - \frac{C_{A^-}^{qe}\beta^-(h)}{D_{A^-}\alpha^-(h)}\right] \quad (14)$$

where $\beta^{\pm}(h) = \int_0^h(-1/2 + 6(y/h - 1/2)^2)e^{\mp\Psi(h,y)}dy$, $\alpha^{\pm}(h) = \int_0^h e^{\mp\Psi(h,y)}dy$, and $\theta = -dh/dx$ is the local slope of the meniscus with respect to the substrate surface. For the sake of simplicity, we will assume θ to be a constant equal to the macroscopic contact angle. We also assume that the rate of the reaction (eq 1) is sufficiently high, so that chemical quasi-equilibrium holds at the interface. Hence, according to eqs A1 and 8, the concentration of charged groups at the interface in eqs 11−14 can be expressed as

$$X_{R^-}(h) = \frac{X_R}{1 + KC_{H^+}^{qe}(h)e^{-\Psi_S(h)}} \quad (15)$$

where $\Psi_S(h) = \Psi(h,0)$ is the quasi-equilibrium electric potential at the interface.

The unknown functions $\Phi(h)$ and $C_i^{qe}(h)$ can be obtained from the set of eqs 11−14 (one of eqs 12−14 can be excluded as the respective concentration can be obtained from eq 10). However, for this purpose, we need to know the quasi-equilibrium potential distribution $\Psi(h,y)$. Making use of the above assumptions, it can be shown[9,11] that $\Psi(h,y)$ can be found from eqs A2, A4, and A5, where the local concentrations $C_i^{qe}(h)$ should be substituted instead of C_i^0. Using the distribution $\Psi(h,y)$, we obtain the functions $\alpha^{\pm}(h)$, $\beta^{\pm}(h)$, and $X_{R^-}(h)$, which have to be substituted in eqs 11−14.

It is important to note that, assuming planar geometry of the air/solution interface (i.e., a constant slope dh/dx at any distance from the contact line), one cannot obtain a steady-state solution of the considered problem because in such a system the concentration and potential profiles should propagate up to infinity. In a real system, the slope dh/dx does not remain constant. It increases significantly at distances on the order of the capillary length. At these distances, the propagation of the concentration and potential profiles becomes much slower, and their further propagation can be neglected for the time scale of a real experiment. Hence, we can assume that the quasi-state profiles extend only up to a certain distance from the contact line, which is on the order of the capillary length. The exact choice of this distance does not significantly affect the results because the most significant change of the ion concentrations and the potential occurs in the regions where the diffuse layers overlap, i.e., at the distances that are smaller than the capillary length by some orders of magnitude.[11] Therefore, for a given finite film thickness, h_m, (Figure 1), we can set the following boundary conditions for eqs 11−14:

$$C_i^{qe}(h_m) = C_i^0 \text{ and } \Phi(h_m) = 0 \quad (16)$$

Thus, to obtain the ion concentrations and the electric potential distributions around the contact line, $C_i(x,y)$ and $\varphi(x,y)$, one should solve first the equation set (eqs 11−14) subject to boundary conditions (eq 16) to find the quasi-equilibrium concentrations $C_i^{qe}(x)$ and the potential $\Phi(x)$. The integration can be performed numerically and should include obtaining the quasi-equilibrium electric potential $\Psi(x,y)$ and surface charge density $\sigma(x)$ for each particular $h(x)$ by using eqs A2, A4, and

A5. Then, using the obtained concentrations $C_i^{qe}(x)$ and potentials $\Psi(x,y)$ and $\Phi(x)$, we can reconstruct the actual ion concentrations and electric potential distributions $C_i(x,y)$ and $\varphi(x,y)$ according to eqs 8 and 9. However, such reconstruction is not always necessary because in some cases the functions $C_i^{qe}(x)$, $\Psi(x,y)$, and $\Phi(x)$ are sufficient to characterize the system, particularly to obtain the partial ion fluxes induced in the subphase during a steady-state monolayer transfer.

An important feature of the above formulated problem is that all system characteristics, which we are looking for, are functions of the ratio U/θ. The steady-state dynamic contact angle is a function of the contact line velocity: $\theta = \theta(U)$. Hence, the ratio $U/\theta(U)$ is a certain function of the velocity U. However, the explicit form of this function is out of the scope of the present study, so that the obtained system characteristics are presented simply as the functions of the ratio U/θ.

3.2. Analysis of Concentrations and Electric Potential Profiles and Partial Ion Fluxes. The curves in Figure 5a,b show the profiles of the quasi-equilibrium counterion concentrations and the potential Φ around the contact line for different deposition rates. As discussed above, near the contact line, the potential-determining counterions, H^+, are removed from the subphase faster than they are supplied by convection. Therefore, their quasi-equilibrium concentration decreases in the vicinity of the contact line (dashed lines in Figure 5a). In contrast, the counterions of the indifferent electrolyte C^+ are not removed from the subphase, but they are continuously supplied to the contact line due to convection. Therefore, their quasi-equilibrium concentration increases toward the contact line (full lines in Figure 5a). The higher the monolayer transfer rate U (or the smaller the angle θ), the sharper the ion concentration profiles. According to eq 8, the ratio of the local concentrations of counterions is defined by the ratio of their quasi-equilibrium concentrations:

$$\frac{C_{H^+}(x,y)}{C_{C^+}(x,y)} = \frac{C_{H^+}^{qe}(x)}{C_{C^+}^{qe}(x)} \tag{17}$$

Hence, in the subphase around the contact line, the potential-determining counterions H^+ are gradually replaced by the counterions of the indifferent electrolyte C^+ as the monolayer transfer rate increases.

The data presented in Figure 5b show the behavior of the potential Φ, which increases in the vicinity of the contact line with reference to the bulk solution. In the considered system, it is determined mainly by the concentration gradient of H^+ ions having the highest diffusion coefficient. In the general case, the potential Φ can be of any sign and it can demonstrate a complex behavior dependent on the subphase composition.[11]

The curves in Figure 5c show the profiles of the ions' electrochemical potentials. According to eqs 8, 9, and 16, they can be calculated as

$$\Delta\mu_i^{el} = RT\left(z_i\Phi + \ln\frac{C_i^{qe}}{C_i^0}\right) \tag{18}$$

As discussed above, the electrochemical potential of H^+ ions around the contact line decreases with respect to that in the bulk solution, whereas the electrochemical potential of the counterions of the indifferent electrolyte C^+ increases.

The formation of concentration and electric potential profiles in the subphase around the contact line leads to the appearance of the ions' electrodiffusion fluxes. These fluxes restore the steady-state balance of ions during the monolayer deposition. The partial ions fluxes are presented in Figure 6. In each cross-section of the film, the total flux of the H^+ ions (curve 3) is composed from their convective (curve 1) and electrodiffusion (curve 2) fluxes and it is equal to the flux of the fatty acid anions R^- transferred with the monolayers, $2UX_{R^-}$ (due to the requirement of electroneutrality of the deposited LB film). Toward the contact line, the concentration of dissociated fatty acid at the interface X_{R^-}, the surface charge, and the total flux of H^+ ions decrease (cf. Figures 4 with Figure 6). This is a result of permanent binding of H^+ ions by charged interfacial groups. However, near the contact line, the convective component of the H^+ ions' flux decreases faster than the total flux because, within a strong overlap of the diffuse layers, the direct

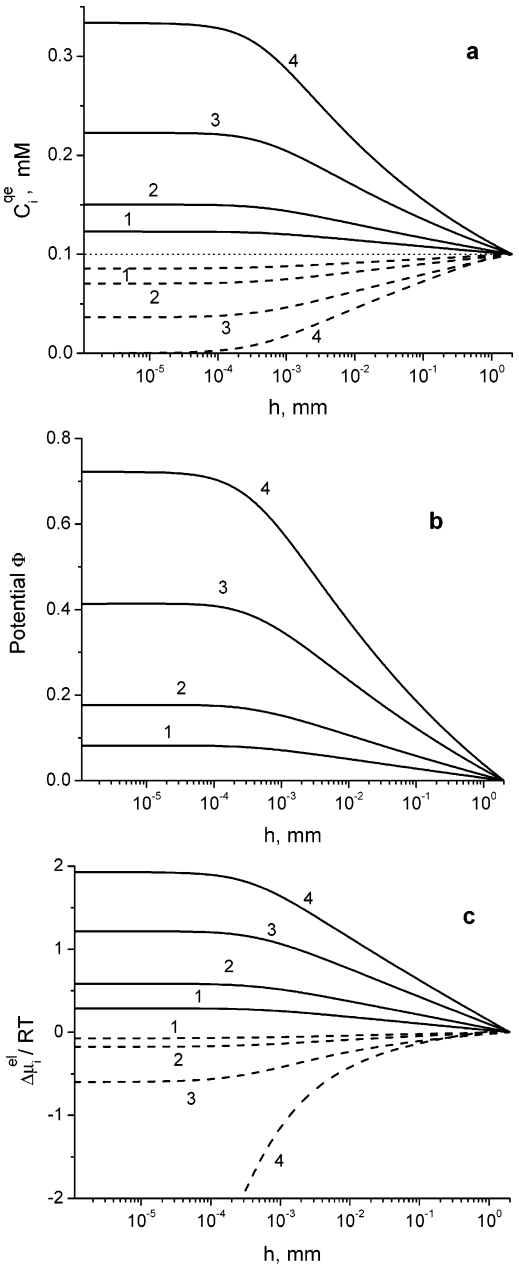

Figure 5. Profiles of quasi-equilibrium concentrations of counterions C^+ (full lines) and H^+ ions (dashed lines) (a), of the potential Φ (b), and of the electrochemical potentials of counterions C^+ (full lines) and H^+ ions (dashed lines) (normalized by RT) (c) in the meniscus region for different deposition rates: $U/\theta = 0.125$ mm/s (1), 0.25 mm/s (2), 0.5 mm/s (3), 0.75 mm/s (4) (pH = 4, $C_{C^+}^0 = 10^{-4}$ M).

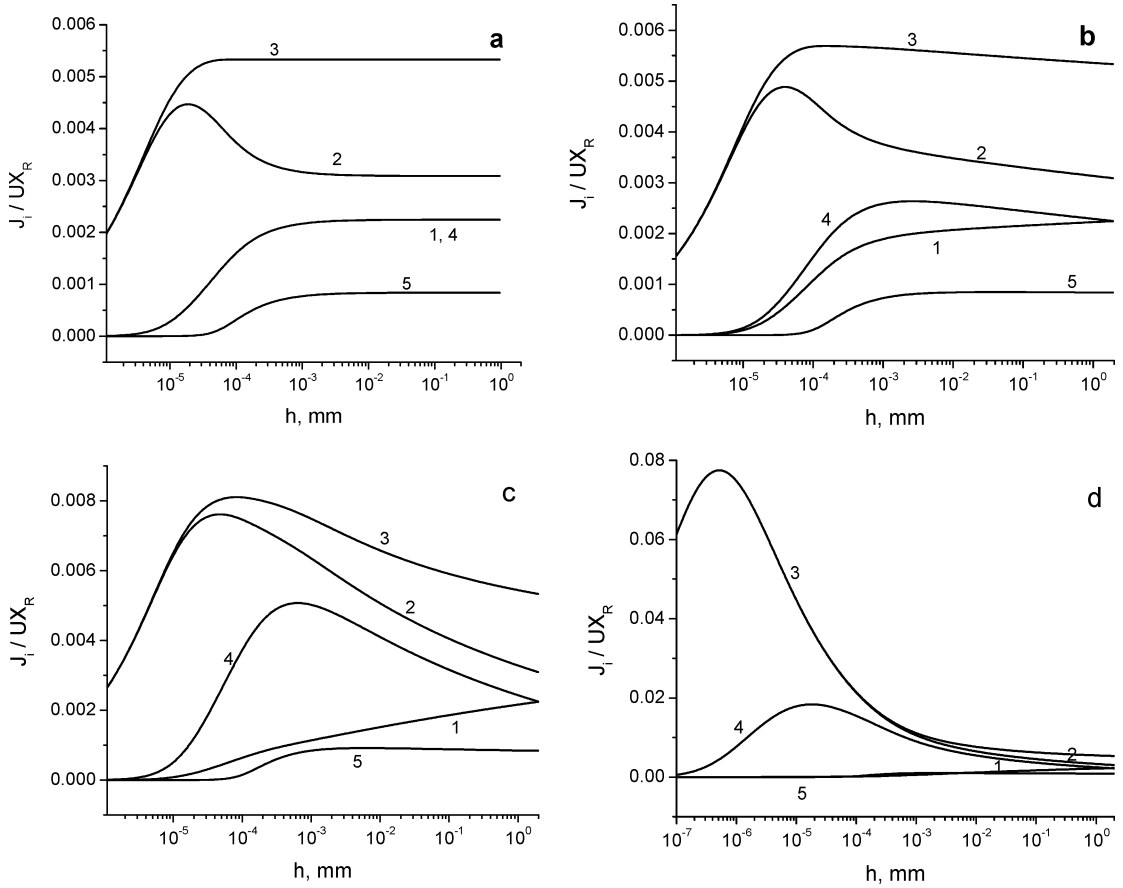

Figure 6. Convective (1), electrodiffusion (2), and total (3) fluxes of H^+ ions and convective fluxes of the cations C^+ (4) and the anions A^- (5) (normalized by $2UX_R$) in the subphase around the contact line vs distance between the interfaces for different deposition rates: $U/\theta = 0$ (infinitely slow deposition) (a), 0.125 mm/c (b), 0.5 mm/c (c), 0.75 mm/c (d) ($C^0_{C^+} = 10^{-4}$ M, pH = 4).

convective flux of the H^+ ions moving close to the surfaces is almost completely compensated for by the opposite flux in the central part of the film. Therefore, in the regions of small film thickness, the required total flux is provided mainly by the electrodiffusion component (Figure 6). As the deposition rate increases, the contribution of the convective component gradually decreases because of an increasing deficit of H^+ ions near the contact line (Figure 5a). Accordingly, the contribution of the electrodiffusion component increases (Figure 6b−d).

Under steady-state conditions, the electrodiffusion fluxes of the cations and anions attributed to the indifferent electrolyte (C^+ and A^-) are completely compensated for by their convective fluxes, and thus, their total fluxes are zero. With increasing deposition rate, the concentration of C^+ ions increases. Simultaneously, their convective and the electrodiffusion fluxes increase to compensate for each other (Figure 6b−d).

3.3. Maximum Deposition Rate. In Figure 7, the behavior of the quasi-equilibrium concentration of the H^+ ions is shown in the immediate vicinity of the contact line. With increasing deposition rate, the concentration $C^{qe}_{H^+}(0)$ decreases and approaches zero. The larger the indifferent electrolyte concentration $C^0_{C^+}$ in the bulk solution, the faster the decrease of $C^{qe}_{H^+}(0)$, because the replacement of the H^+ ions by C^+ ions near the contact line becomes faster (larger convective flux of C^+ ions requires larger electrodiffusion flux). It is important that the above formulated problem does not have a steady-state solution for the velocities U larger than the critical one for which the concentration $C^{qe}_{H^+}(0)$ approaches zero. For higher velocities of the interfaces, the electrodiffusion flux of H^+ ions is insufficient

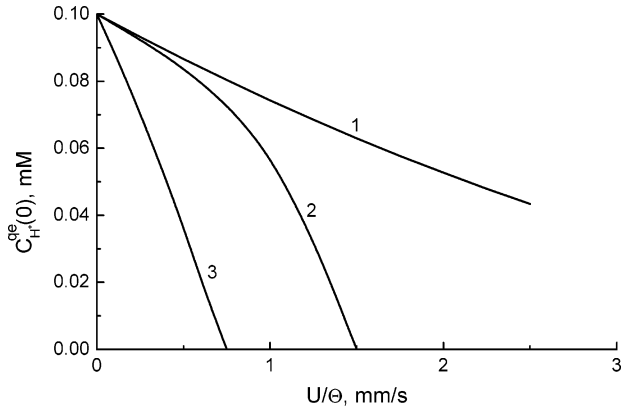

Figure 7. Variation of the quasi-equilibrium concentration of H^+ ions in the immediate vicinity of the contact line with the deposition rate for different subphase compositions: $C^0_{C^+} = 0$ (1), $C^0_{C^+} = 10^{-6}$ M (2), $C^0_{C^+} = 10^{-4}$ M (3); pH = 4.

to completely compensate for the negative charge transferred with the monolayers.

According to eq 15, the surface charge density near the contact line increases with the deposition rate (Figure 8). Such a behavior takes place due to the local decrease in concentration of the potential-determining H^+ ions. In turn, the increasing surface charge density requires a larger electrodiffusion flux of H^+ ions in the subphase and therefore still smaller concentrations ($C^{qe}_{H^+}(0)$). When the transfer velocity U becomes close to the critical one, the surface charge density increases dramatically. This results in a stronger double layer electrostatic repulsion

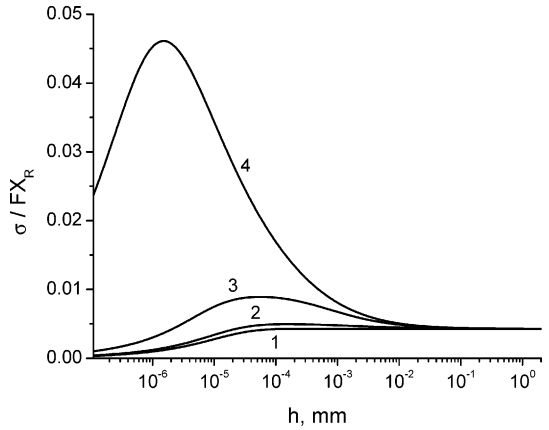

Figure 8. Variation of the surface charge density (normalized by FX_R) in the meniscus region for different deposition rates: $U/\theta = 0$ (1), 1.0 mm/s (2), 1.4 mm/s (3), 1.5 mm/s (4) (pH = 4, $C_C^{+0} = 10^{-6}$ M).

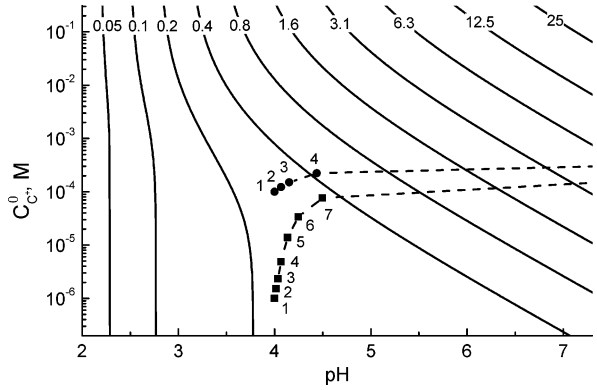

Figure 9. Effect of concentrations $C_{H^+}^0$ and $C_{C^+}^0$ on the electrostatic repulsion energy between two monolayers. The full lines are the lines of constant repulsion energy corresponding to (left to right) ΔG_{el} = 0.05, 0.1, 0.2, 0.4, 0.8, 1.6, 3.1, 6.3, 12.5, and 25 mJ/m^2. The dashed lines show the variation of local subphase composition at the contact line with the deposition rate for initial concentrations $C_{H^+}^0 = 10^{-4}$ M, $C_{C^+}^0 = 10^{-4}$ M (●) and $C_{H^+}^0 = 10^{-4}$ M, $C_{C^+}^0 = 10^{-6}$ M (■). The points correspond to the deposition rates: $U/\theta = 0$ (infinitely slow deposition) (1), 0.125 mm/c (2), 0.25 mm/c (3), 0.5 mm/c (4), 0.75 mm/c (5), 1.0 mm/c (6), and 1.25 mm/c (7).

between the interfaces and a disruption of the deposition process with further velocity increase.

For a system containing only monovalent ions, the electrostatic repulsion energy between two charged monolayers coming in contact can be obtained as[8,21,22]

$$\Delta G_{el} = RTX_R \ln(1-\alpha) - \frac{4}{F}[2(RT)^3\epsilon\epsilon_0(C_{H^+}^0 + C_{C^+}^0)]^{1/2}\left(\cosh\frac{\varphi_S}{2} - 1\right) \quad (19)$$

where $\alpha = X_{R^-}/X_R$ is the degree of dissociation and φ_S is the normalized (by F/RT) electric potential at the interface for a single monolayer in equilibrium with the given solution. The effect of concentrations $C_{H^+}^0$ and $C_{C^+}^0$ on the electrostatic repulsion energy can be seen from Figure 9.

Under dynamic conditions, the local quasi-equilibrium concentrations in the immediate vicinity of the contact line are very different from those in the bulk solution (Figure 5). Although the equilibrium is absent as a whole in the system, the local quasi-equilibrium can hold within a sufficiently small part of the system.[8,11] Accordingly, the interaction energy, respective of the work of adhesion, can be calculated, which, due to local equilibrium, should be related to the local subphase composition at the contact line. Being the functions of local concentrations, they should change under dynamic conditions. The calculations of total interaction energy meet difficulties because there are some open questions concerning its components.[8,16,23] It is clear, however, that the total interaction energy should increase (and the adhesion work should decrease) when the electrostatic repulsion energy increases. Under dynamic conditions, the electrostatic repulsion energy can be obtained from the same eq 19 by using quasi-equilibrium concentrations at the contact line instead of bulk concentrations, provided that local quasi-equilibrium holds. With increasing velocity (U), the quasi-equilibrium concentration of H^+ ions decreases and that of C^+ ions increases; accordingly, the electrostatic repulsion energy increases. It is seen from Figure 9 that in the presence of an indifferent electrolyte such increases can be rather high, much higher than without indifferent electrolytes.[8] Such an increase may be sufficient to disrupt the deposition process.

It might appear that such an equilibrium thermodynamic parameter as the adhesion work, W_{adh}, cannot be employed for characterizing the behavior of the dynamic three-phase contact zone. However, when considering sufficiently weak driving forces violating the equilibrium and corresponding very small parts of the entire system, one can see that equilibrium is only slightly violated within such small system parts. Consequently, such small parts are considered to be in local quasi-equilibrium and can be described on the basis of a thermodynamic approach. In particular, for such a description, one employs physical quantities defined within the framework of the rigorous equilibrium thermodynamics such as, pressure, chemical potentials, temperature, etc. For analyzing multiphase flows, a modification of the above concept has been often introduced.[24] Accordingly, it is assumed that the interface and the adjacent parts of the contacting phases are in the quasi-equilibrium state. The latter assumption allows use of the relationships of the interfacial thermodynamics with respect to the quantities attributed to the interface and to its close vicinity, e.g., dynamic surface tension, disjoining pressure in thin liquid film dynamics, etc. (see, for example, ref 24).

Accordingly, a quasi-equilibrium adhesion work can be introduced as a function of the subphase composition in the immediate vicinity of the interface. The adhesion work is defined by the interactions (molecular, electrostatic, etc.) between the monolayer molecules and the substrate surface. These interactions are dependent on the subphase composition within the region around the contact line where the surface forces are acting. As this region is very small, one can expect that the quasi-equilibrium establishes rapidly and holds in this region despite irreversible conditions. Thus, quasi-equilibrium adhesion work is defined by the change of the free energy but under the conditions when two interfaces are put together in a subphase with the same composition as in the immediate vicinity of the contact line. There are no doubts that, also under dynamic conditions, a decrease in the adhesion work leads to a decrease in the contact angle. However, it should be noted that, in contrast to the equilibrium case, the Young equation is not valid under dynamic conditions.

When, in experiments, the substrate velocity U exceeds a critical value, the deposited monolayer begins to entrain a film of liquid.[12−16] Probably, the critical velocity determined from the condition of zero adhesion work[9−11] should be somewhat different from that predicted from the condition of zero

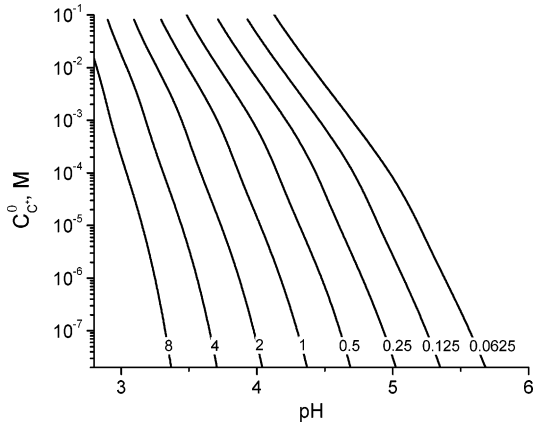

Figure 10. Diagram of the maximum deposition rate for a fatty acid monolayer in the presence of an indifferent electrolyte. The lines of constant maximum deposition rate (left to right) correspond to $U/\theta =$ 8, 4, 2, 1, 0.5, 0.25, 0.125, and 0.0625 mm/s.

concentration $C^{qe}_{H^+}(0)$. However, these two critical velocities should be close to each other because of a very rapid increase of the monolayer charge when the substrate speed is close to the critical value (Figure 8). We have to also keep in mind that the contact angle θ also decreases with decreasing adhesion work. As a result, the ratio $U/\theta(U)$ increases faster than the substrate velocity U. This leads to a much more rapid decrease of the concentration $C^{qe}_{H^+}(0)$ and an increase of the monolayer charge when the substrate speed approaches the critical value.

In the diagram presented in Figure 10, maximum deposition rates for a fatty acid monolayer were determined from the condition of zero concentration $C^{qe}_{H^+}(0)$. According to this diagram, for a given rate, the monolayer deposition is possible from the subphases, the composition of which corresponds to the points left and below the respective curve. For a given indifferent electrolyte concentration in the bulk solution $C^0_{C^+}$, the maximum deposition rate decreases with increasing pH. Such a trend is in line with the experimental data.[12−15] For a given bulk pH, the maximum deposition rate decreases with increasing indifferent electrolyte concentration $C^0_{C^+}$. Thus, the bad monolayer deposition, which is observed in the presence of indifferent electrolytes[12,13,15,17,] may be explained through the replacement of the potential-determining H^+ ions within the diffuse layers by the cations C^+, as discussed above. These quantitative results support the qualitative conclusions that were obtained in our previous study based on the monolayer behavior only at small deposition rates.[10]

When indifferent electrolytes are absent,[11] the system behavior differs substantially from that predicted in the present paper. However, in systems without indifferent electrolytes, concentration polarization is also observed; this leads to a very small increase of the monolayer charge. For such a case, a decrease of local quasi-equilibrium concentrations of the potential-determining ions is compensated for by a respective increase of the local quasi-equilibrium potential Ψ. Therefore, the increase of the electrostatic repulsion energy turns out to be relatively small.[8] Probably, such a small increase of the repulsion is insufficient for the explanation of the observed decrease in the adhesion work.[11] However, the increase of the monolayer charge becomes possible, even if very small amounts of indifferent electrolytes are present in the subphase. For example, the results presented in Figure 8 show that a significant increase of the surface charge density is possible in the presence of 10^{-6} M of the cations (C^+).

It should be also noted that, according to the model considered here, the quasi-equilibrium concentrations of potential-determining counterions (H^+ or Cd^{2+}) near the contact line approach very small, but nonzero, values if indifferent electrolytes are absent in the solution.[11] In this case, the critical velocity can be determined only from the condition of zero adhesion work. In the presence of indifferent electrolytes, the concentration $C^{qe}_{H^+}(0)$ can approach zero (Figure 7), and the corresponding evaluation gives a reasonable prediction for the critical velocity.

It is necessary to note that, at very small concentrations of H^+ ion, the dissociation of water molecules (the so-called "water-splitting" effect) can influence the processes around the contact line.[8,9,11] During the deposition, the monolayer can bind H^+ ions that appear in the solution due to water dissociation, and the remaining hydroxyl ions should be transferred to the bulk solution by both convection and the electrodiffusion mechanism. Such a change of the chemical environment near the contact line should also influence the monolayer interaction with the substrate and additionally complicate the deposition process. Nevertheless, dissociation of water should not play a significant role in the presence of an indifferent electrolyte.

4. Conclusions

The analysis of steady-state ion balance in the solution around the three-phase contact line during the deposition of charged Langmuir monolayers allows the prediction of local changes in the subphase composition and in the electric potential distribution. Such changes influence the deposition process, particularly the monolayer adhesion work and the maximum deposition rate. If indifferent electrolytes are present in the solutions, they can affect the surface charge and the electric potential distributions and therefore the overall deposition process.

The mathematical model developed in ref 11 can also be applied for the description of systems containing indifferent electrolytes at any deposition rate up to the critical one. The analysis of ion concentration profiles shows that the quasi-equilibrium concentration of the potential-determining counterions decreases toward the contact line, whereas that of the indifferent electrolyte counterions increases. With increasing deposition rate, the indifferent electrolyte counterions gradually replace the potential-determining counterions in a close vicinity to the contact line. This leads to the increase of both monolayer ionization and electrostatic repulsion between the monolayers. A comparison of systems with and without indifferent electrolytes shows that, in the absence of indifferent electrolytes, a significant increase of the monolayer ionization becomes impossible. However, even the presence of small amounts of indifferent electrolytes results in a significant increase of the monolayer charge with increasing deposition rate.

The charge of the monolayer increases dramatically when the deposition rate approaches the critical value, and electrostatic repulsion can disrupt the monolayer deposition with a further increase of the substrate velocity. For substrate velocities larger than the critical one, the electrodiffusion ions fluxes cannot restore the steady-state ion balance in the solution around the three-phase contact line and stationary monolayer deposition is impossible. The maximum deposition rate depends on the subphase ionic composition. It decreases with increase of both pH and indifferent electrolyte concentration in the bulk solution. The obtained results are in agreement with the known experimental data.

Acknowledgment. Financial assistance by the Bundesministerium für Bildung, Wissenschaft, Forschung, and Technologie

(BMBF) of Germany and the Ukrainian Ministry of Education and Science (joint project UKR 02/013). The National Ukrainian Academy of Sciences (project 9-003) is gratefully acknowledged.

Appendix

For the reaction given by eq 1, the equilibrium condition can be written as

$$X_{RH} = KX_{R^-}C^S_{H^+} \tag{A1}$$

where X_{R^-} and X_{RH} are the interfacial molar concentrations of the dissociated and nondissociated fatty acids (R^- and RH, respectively), $C^S_{H^+}$ is the bulk molar concentration of the cations (H^+) in the immediate vicinity of the interface, and K is the equilibrium constant. For the system under consideration, the equilibrium surface charge density can be expressed as[10,18]

$$\sigma = -FX_{R^-} = -\frac{FX_R}{1 + KC^0_{H^+}e^{-\varphi_S}} \tag{A2}$$

where $X_R = X_{R^-} + X_{RH}$ is the total amount of fatty acid at the interface, $C^0_{H^+}$ is the molar concentration of the cations (H^+) in the bulk solution far from the interface, φ_S is the normalized (by F/RT) electric potential at the interface, F is the Faraday constant, R is the gas constant, and T is the absolute temperature. In equilibrium, the ion concentrations within the diffuse parts of the electrical double layers (DL) formed at charged interfaces can be represented using the Boltzmann distribution

$$C_i = C^0_i e^{-z_i\varphi} \tag{A3}$$

where z_i and C^0_i are the ith ion charge and concentration in the bulk solution far from the interface, respectively, and φ is the normalized electric potential.

In the solution adjacent to the contact line, the diffuse parts of DL, which are formed at the monolayer and at the substrate surface, overlap. Therefore, the electric potential increases in this region, whereas the surface charge density decreases.[9−11,19] The equilibrium electric potential distribution in the vicinity of the contact line can be obtained from the solution of the Poisson−Boltzmann equation with the respective boundary conditions taking into account the charge regulation at the interfaces (eq A2). Considering small contact angles, we can simplify the problem. In this case, the potential distribution within the thin liquid film between the charged monolayer and the substrate surface (Figure 1) can be approximately calculated as for a flat-parallel system:[10]

$$\varphi = \varphi_0 + 2\ln\left\{\mathrm{sn}\left[\tilde{K}(k) - \frac{\kappa}{2}\left|\frac{h}{2} - y\right|\exp\left(-\frac{\varphi_0}{2}\right), k\right]\right\} \tag{A4}$$

where $h = h(x)$ is the local film thickness slowly changing with the x-coordinate, directed along the film (normal to the contact line), y is the coordinate directed normal to the film surfaces ($0 \le y \le h$), φ_0 is the dimensionless electric potential in the symmetry plane ($y = h/2$), $\mathrm{sn}(t,k)$ is the elliptic function with the modulus $k = \exp\varphi_0$, $\tilde{K}(k)$ is the quarter period of the elliptic function, $\kappa = \sqrt{2F^2(C^0_{H^+}+C^0_{C^+})/\epsilon_0\epsilon RT}$ is the inverse Debye length, ϵ is the dielectric constant, and ϵ_0 is the permittivity of vacuum. The surface charge density for the considered system can be expressed as[10,18]

$$\sigma = -[4\epsilon_0\epsilon RT(C^0_{H^+} + C^0_{C^+})(\cos h\,\varphi_S - \cos h\,\varphi_0)]^{1/2} \tag{A5}$$

Substitution of $y = 0$ or $y = h$ into eq A4 leads to an equation for the dimensionless surface potential φ_S. Combining this equation with eqs A2 and A5, we obtain a set of transcendent equations for obtaining all the three unknowns φ_S, φ_0, and σ. The solution gives us these variables as functions of the local film thickness h (which is a function of the distance to the contact line $h = h(x)$) and the bulk concentrations $C^0_{H^+}$ and $C^0_{C^+}$.

For the sake of simplicity, we consider here a symmetrical film; i.e., we assume that the substrate surface is covered by the same monolayer previously deposited (Y-type mode of LB deposition) and that the monolayer transfer ratio is close to unity. Also, we assume that the monolayer is in close-packed condensed state. The latter means that the value X_R is nearly independent of both surface pressure and solution pH. Thus, we can set approximately $X_R = 8.3 \times 10^{-6}$ mol/m^2 that gives a typical value for fatty acid monolayers.[19] For the equilibrium constant, we take the same value as in our previous studies:[9−11] $K = 6.54 \times 10^4$ dm^3/mol.

References and Notes

(1) Gleiche, M.; Chi, L. F.; Fuchs, H. *Nature* **2000**, *403*, 173−175.

(2) Moraille, P.; Badia, A. *Langmuir* **2002**, *18*, 4414−4419. Moraille, P.; Badia, A. *Langmuir* **2003**, *19*, 8041−8049.

(3) Purrucker, O.; Förtig, A.; Lüdtke, K.; Jordan, R.; Tanaka, M. *J. Am. Chem. Soc.* **2005**, *127*, 1258−1264.

(4) Huang, J.; Tao, A. R.; Connor, S.; He, R.; Yang, P. *Nano Lett.* **2006**, *6*, 524−529.

(5) Howland, M. C.; Johal, M. S.; Parikh, A. N. *Langmuir* **2005**, *21*, 10468−10474.

(6) Chen, X.; Lu, N.; Zhang, H.; Hirtz, M.; Wu, L.; Fuchs, H.; Chi, L. F. *J. Phys. Chem. B* **2006**, *110*, 8039−8046.

(7) Mahnke, J.; Vollhardt, D.; Stöckelhuber, K. W.; Meine, K.; Schulze, H. J. *Langmuir* **1999**, *15*, 8220−8224.

(8) Kovalchuk, V. I.; Bondarenko, M. P.; Zholkovskiy, E. K.; Vollhardt, D. *J. Phys. Chem. B* **2003**, *107*, 3486−3495.

(9) Kovalchuk, V. I.; Bondarenko, M. P.; Zholkovskiy, E. K.; Vollhardt, D. *J. Phys. Chem. B* **2004**, *108*, 13449−13455.

(10) Kovalchuk, V. I.; Bondarenko, M. P.; Zholkovskiy, E. K.; Vollhardt, D. *J. Adhes.* **2004**, *80*, 851−870.

(11) Bondarenko, M. P.; Zholkovskiy, E. K.; Kovalchuk, V. I.; Vollhardt, D. *J. Phys. Chem. B* **2006**, *110*, 1843−1855.

(12) Petrov, J. G.; Kuhn, H.; Möbius, D. *J. Colloid Interface Sci.* **1980**, *73*, 66−75.

(13) Petrov, J. G. *Z. Phys. Chem. (Leipzig)* **1985**, *266*, 706−712.

(14) Petrov, J. G. *Colloids and Surf.* **1986**, *17*, 283−294.

(15) Veale, G.; Peterson, I. R. *J. Colloid Interface Sci.* **1985**, *103*, 178−189.

(16) Petrov, J. G.; Angelova, A. *Langmuir* **1992**, *8*, 3109−3115.

(17) Hasmonay, H.; Vincent, M.; Dupeyrat, M. *Thin Solid Films* **1980**, *68*, 21−31.

(18) Israelachvili, J. N. *Intermolecular and surface forces*; Academic Press: London, 1997.

(19) Kovalchuk, V. I.; Bondarenko, M. P.; Zholkovskiy, E. K.; Vollhardt, D. *J. Phys. Chem. B* **2001**, *105*, 9254−9265.

(20) de Gennes, P. G. *Colloid Polym. Sci.* **1986**, *264*, 463−465.

(21) Payens, Th. A. J. *Philips Res. Rep.* **1955**, *10*, 425−481.

(22) Helm, C. A.; Laxhuber, L.; Lösche, M.; Möhwald, H. *Colloid Polym. Sci.* **1986**, *264*, 46−55.

(23) de Feijter, J. A.; Vrij, A. *J. Colloid Int. Sci.* **1979**, *70*, 456−466.

(24) Edwards, D.A.; Brenner, H.; Wasan, D.T. *Interfacial Transport Processes and Rheology*; Butterworth-Heinemann, Boston, 1991.